

Diffuse Gas Condensation Induced by Variations of the Ionizing Flux

Antonio Parravano¹ and Catherine Pech²

¹ Centro de Astrofísica Teórica, Facultad de Ciencias, Universidad de Los Andes,
A. Postal 26 La Hechicera, Mérida 5251, Venezuela.

² Institut National des Sciences Appliquées de Toulouse, France.

Received ???; accepted ???

Abstract. The variation of an ionizing flux as a mechanism to stimulate the condensation of a diffuse gas is considered. To illustrate this effect, two situations are examined: one on the context of pregalactic conditions, and the other on the context of the actual interstellar medium. We focus our attention on flash-like variations; that is, during a “short” period of time the ionizing flux is enhanced in comparison to the pre- and post-flash values. In both cases the cause of the induced phase change is the same: the enhancement of the cooling rate by the increase in the electron density caused by the momentary increase of ionizing flux. After the passing of the flash, the cooling rate remains enhanced due to the “inertia of the ionization”. In the first case (metal free gas) the cooling rate is enhanced due to the fact that the increase of the electron density makes possible the gas phase formation of H_2 by the creation of the intermediaries H^- and H_2^+ . We show that after the passing of the photo-ionizing flash a cloud near thermo-chemical equilibrium at ~ 8000 K may be induced to increase its H_2 content by many orders of magnitude, causing a rapid decrease of its temperature to values as low as 100 K. In the second case (solar abundances gas) the dominant cooling mechanism of the warm neutral gas (the excitation of heavy ions by electron impacts) is proportional to the electron density. We show that, for the expected states of the warm interstellar gas, ionizing flashes may induce the phase transition from the warm to the cool phase. The results indicate that the mechanism of induced condensation studied here might play a relevant role in the gas evolution of the diffuse gas in both, the pregalactic and the actual interstellar medium conditions.

Key words: Plasmas - Galaxy: formation - ISM: general

1. Introduction

Thermal condensation of diffuse gas is a commonly invoked route for the formation of dense astrophysical structures. This thermal condensation may occur spontaneously or may be induced by variations of the external conditions. In the first situation (spontaneous condensation), the initially diffuse gas is in a state out of equilibrium in which the cooling dominates over the heating. Eventually, the gas reaches a thermo-chemical equilibrium in a dense and cool state. In the second situation (induced condensation), in absence of variation of external conditions the gas would reach (or be in) a state of thermo-chemical equilibrium in a diffuse and hot state, but in presence of appropriate variations of the external conditions, the gas evolves toward a cooler and denser state. Induced condensation of diffuse gas must play an important role in the large scale evolution of the medium; specially if the stimulating sources are able to induced condensation far away from them. The synchronization and the large scale patterns of star formation may be governed by this kind of stimulation. In fact, most of the models and numerical simulations of the star formation in disk galaxies include as a main process the so-called self-propagating star formation (Gerola & Seiden 1978; Seiden & Gerola 1982;

Send offprint requests to: A. Parravano

Shore 1981, 1983; Palouš et al. 1990; Comins & Shore 1990; Cammerer & Shchekinov 1994). This kind of systems are part of the wider class of reaction-diffusion systems (Kapral 1993, and references therein). In particular, the so-called exitable media are appropriate to capture the main features of the pattern formation in disk galaxies (Smolin 1996).

Among the external conditions whose variations would induce phase transitions are the external pressure and the ionizing flux. We focus our attention on the effect of the variation of the ionizing flux, keeping in mind that induced condensation by pressure variations may play a relevant role (Roberts 1969; Shapiro & Kang 1987). In particular, we focus our attention on flash-like variations; that is, during a "short" period of time, the ionizing flux is enhanced in comparison to the pre- and post-flash values. To illustrate this mechanism of induced condensation, two examples are given here: one on the context of pregalactic conditions (in a free metal cloud), and the other on the context of the actual interstellar medium (in a gas with solar abundances). In both cases the cause of the induced phase change is the same: the increase in the electron density due to the momentary increase of ionizing flux enhances the cooling rate. After the passing of the flash, the cooling rate remains enhanced due to the inertia of the ionization (i.e. the characteristic recombination time is much larger than the cooling one).

Many scenarios in which a flash of radiation affects the evolution of gas clouds can be imagined. For the metal free gas case, this kind of induced condensation might be relevant at the epoch of galaxy formation. In particular, the ionizing flash effect might be a key step in the sequence of events that have conduced to the formation of globular clusters. It has been stated by Cox (1985) that "such a rapid fragmentation of the halo almost certainly requires inducement by energy leaving the (primitive) disk". For the case of a gas with solar abundances, the evoked mechanisms of induction are diverse but generally associated to compression and convergent mass flows (see review by Elmegreen 1992). However, in addition to these mechanisms, the induced condensation by ionizing flashes appears as an effect to be considered.

In Sec. 2 the basic equations to follow the thermal and chemical evolution of a gas subject to variations of the gas pressure and the ionizing flux are given. In Sec. 3 the evolution of a free metal gas cloud subject to a flash of ionizing and dissociating radiation is analyzed, whereas, in Sec. 4, the evolution of a solar abundance gas subject to a flash of cosmic ray flux is considered. Finally, the conclusions are given in Sec. 5.

2. Basic equations

The thermal and chemical evolution of a gas subjected to variable external conditions are calculated by solving the system of kinetic equations and the equation of energy conservation. The system of kinetic equations can be written in the general form

$$\begin{aligned} \frac{dX_i}{dt} = n \left(\sum_{j,k} \alpha_{jk} X_j X_k - X_i \sum_l \alpha_{il} X_l \right) \\ + \sum_m \alpha_m X_m - \alpha_i X_i, \end{aligned} \quad (1)$$

where n is the total number density of hydrogen nuclei and X_i is the relative number density of the i -th species. In Eq. (1), α_{jk} and α_{il} are, respectively, the formation and destruction rates of the i -th species due to double collisions, whereas, α_m and α_i are, respectively, the production and destruction rates of the i -th species due to the interaction of particles with radiation.

The equation of energy conservation equation can be expressed as

$$\frac{dU}{dt} + P \frac{dV}{dt} + \mathcal{L} = 0, \quad (2)$$

where U is the internal energy by unit mass, \mathcal{L} is the net cooling rate by unit mass ($\mathcal{L} = (\Lambda - \Gamma)/\rho$), P is the pressure, ρ is the mass density, and V is the specific volume. Assuming that $P = \rho RT/\mu$ and $U = 3RT/2\mu$, with R the gas constant, and μ the molar mass, eq. (2) can be written as

$$\frac{dT}{dt} = \frac{T}{\mu} \frac{d\mu}{dt} + \frac{2}{5} \frac{T}{P} \frac{dP}{dt} - \frac{2}{5} \frac{\mu}{R} \mathcal{L}. \quad (3)$$

Two extreme situations that can be used to confine intermediate situations are the constant density and constant pressure approximations. In these approximations, the energy conservation equation can be expressed as

$$\frac{dT}{dt} = \frac{T}{\mu} \frac{d\mu}{dt} - \lambda \frac{\mu}{R} \mathcal{L}, \quad (4)$$

where, $\lambda = 2/3$ or $2/5$ in the constant density or in the constant pressure approximations, respectively.

Variations of the external ionizing sources flux produces direct variation on the rates α_m and α_i , and on the heating rate Γ , whereas, variations of the pressure affect density and temperature. Notice that variations of n or α_i provoke a variation of the chemical state of the gas, and therefore produce a variation of the cooling rate Λ . In the following, we solve the basic equations (1) and (2) with the appropriate assumptions in order to model: a) the evolution of a metal free cloud subjected to a variation of the ionizing and dissociating flux (sec. 3), and b) the evolution of a solar abundance gas subjected to variations of the primary ionization rate due to cosmic rays (sec. 4).

3. Photo-ionizing radiation flash as trigger of efficient H_2 cooling in free metal gas clouds

In the context of formation of galaxies and globular clusters, the non-equilibrium formation of H_2 has been identified as a key process for achieving a rapid cooling below 10^4K (Palla & Stahler 1983; Izotov & Kolesnik 1984; Shapiro & Kang 1987; Palla & Zinnecker 1987; Kang et al. 1990; Anninos et al. 1996; Padoan et al. 1996; Tegmark et al. 1996). On the other hand, the ionization and dissociation of primordial gas by UV background radiation have been taken into account as an important parameter in many studies of the thermo-chemical evolution of pregalactic and intergalactic structures (Kang et al. 1990; Donahue & Shull 1991; Ferrara & Giallongo 1996; Haardt & Madau 1996; Navarro & Steinmetz 1996; Mucket & Kates 1997). In general, the UV background radiation acts as an inhibitor of H_2 formation. However, there are exceptions to this rule. Recently Haiman et al. (1996) have shown that UV background radiation can enhance the formation of H_2 in primordial gas at high densities ($\geq 1\text{cm}^{-3}$) and low temperatures ($\leq 10^4\text{K}$); but for densities lower than the above value, the effect of a *constant* UV background radiation is to inhibit the H_2 formation. As it will be shown in the present section, rapid variations of the UV background radiation can also enhance the non-equilibrium formation of H_2 . In particular, we focus our attention on flash like variations capable of heating and increasing the ionization fraction of an initially warm-neutral gas cloud near thermo-chemical equilibrium. After the passing of the radiation pulse, the enhanced ion fraction makes the gas phase formation of H_2 molecules possible by the creation of the intermediaries H^- and H_2^+ . The presence of small quantities of H_2 molecules then makes possible further radiative cooling to temperatures as low as $\sim 10^2\text{K}$. The rapid cooling (~ 0.2 free-fall times) abruptly reduces the Jeans mass by a factor $\sim 10^4$, permitting the fragmentation of clouds initially marginally stable. Izotov (1989) has considered the homogeneous contraction approach of a gravitational unstable cloud, but here we are interested in delimiting the necessary conditions that provoke the rapid cooling of the cloud without invoking the gravitational collapse. UV radiation pulses have similar effects than shock waves because the post-shock flow also recombines out of equilibrium.

The spectrum, amplitude and duration of the radiation pulse are free parameters in our model. However, it should be noticed that, in order to induce efficient H_2 cooling in the cloud, the detailed form of the flash is not important as long as that, during the flash, the ionization of the cloud increases appreciably and after this, the ionizing flux decreases to background values in a short time compared to the recombination time.

The initial conditions of the cloud and the characteristics of the hypothetical ionizing pulse depend on the chosen scenery. For example in the Fall and Rees (1985) scenery, during the proto-galactic collapse, if the gas is assumed to be lumpy, the overdense regions will cool more rapidly than the underdense regions producing a two-phase medium. But the developing rate of this overdense regions depends on the initial conditions (i.e. the denser regions develop faster; Murray and Lin 1990) and on their interaction with the system. Thus, a dependence of the density contrast and of the mean cloud masses on the galactocentric distance are expected. The assumption of an ionizing flash produced in the galactic nucleus implicitly assumes a radial increment of the delay in the evolution of the clouds relative to the center. The dilution and attenuation of the ionizing and dissociating radiation produced in the flash also introduce a radial dependence. In fact, the possibility that proto-galactic structures are exposed to UV radiation emitted by massive young stars or an active galactic nucleus has been considered previously (Kang et al. 1990). Therefore, it would be useful to know the dependence of the cloud evolution on the flash characteristics, and on the cloud initial state (i.e. cloud mass (M_c), temperature (T), number density (n), and the relative number density of the species (X_i)).

To follow the thermal and chemical evolution of a metal-free cloud in presence of a variable radiation flux, we consider an idealized uniform cloud. The gas model adopted for this application considers the following 9 species: H , H^+ , e , H^- , H_2^+ , H_2 , H_e , H_e^+ , and H_e^{++} . Assuming a mass fraction y ($= 0.3$) of Helium relative to Hydrogen, then $\mu = (1+y)/(1+X_e - X_{H_2} - X_{H_2^+} + y/3.97)$, where X_i is the ratio of the number density of species i to the total number density of Hydrogen nuclei n . The processes of formation and destruction of these nine species are assumed to be the 24 reactions in Table I of Rosenzweig et al. 1994. The adopted cooling rates, include: 1) the collisional ionization of H by electron impact; 2) the free-free transitions of H^+ (Izotov (1989) and references therein); 3) the collisional ionization by electron impact of H_e and H_e^+ ; 4) the free-free transitions of H_e^+ and H_e^{++} ; 5) the total dielectronic cooling rate of H_e^+ (Shapiro & Kang 1987); 6) the H_2 cooling rates due to rotational and vibrational transitions excited by ($H - H_2$) and ($H_2 - H_2$) collisions, calculated according to Lepp and Shull (1983). These H_2 cooling rates must be multiplied

by a factor $L(\tau_{vib})$ and $L(\tau_{rot})$ to take into account the escape probability of the vibrational and rotational photons, respectively. Finally, 7) the excitation of the H_2 vibrational levels ($v \leq 4$) by low energy electron-impact was taken into account (Klonover & Kaldor, 1979).

The external radiation flux affects the photoionization of the Hydrogen and Helium, and the H_2 photo-dissociation (and its associated heating rates; see Rosenzweig et al. 1994). The external photon flux is assumed to have the quasar-like distribution (Shapiro and Kang 1987)

$$\mathcal{N}(\nu, t) = 4.6 \times 10^{-11} \epsilon(t) \left(\frac{\nu}{\nu_H} \right)^{-1.7} \text{ cm}^{-2} \text{ Hz}^{-1} \text{ s}^{-1}, \quad (5)$$

where ν_H is the H Lyman-edge frequency. The function $\epsilon(t)$ is introduced to represent the changes of the flux level outside the cloud, and is assumed to behave as $\epsilon_{ion}(t)$ in the Lyman continuum, and as $\epsilon_{dis}(t)$ for the photo-dissociating photons. Since a homogeneous cloud is assumed in this application, the optical depth at its center, for the ionizing radiation, can be written as:

$$\tau_\nu = 6.6 \times 10^{18} n (\sigma_\nu^H X_H + \sigma_\nu^{H_e} X_{H_e} + \sigma_\nu^{H_e^+} X_{H_e^+}) \left(\frac{M}{n} \right)^{1/3} \quad (6)$$

where M is the mass of the cloud in units of M_\odot and σ_ν^i are the absorption cross sections of species i at frequency ν . As a first approximation, the attenuation of the external radiation field $\mathcal{N}(\nu, t)$ by the factor $\exp^{-\tau_\nu}$ is adopted to schematize the opacity effects. For the dissociating radiation field a similar approximation is adopted (Rosenzweig et al. 1994). Obviously, by using this first approximation, the effect of the ionizing radiation is minimized, and the study of the internal structure of the cloud is not possible.

For the time dependence of the flux level ϵ we assume a flash like variation. More precisely, during a first period of integration the external radiation flux remains at the assumed background value (i.e. $\epsilon_{ion} = \epsilon_{dis} = \epsilon_0$). The duration of this initial period of integration is large enough (i.e. $\sim 10^8$ yr) to ensure that the cloud is near its thermo-chemical equilibrium state. After this first period of stabilization, it is assumed that both, ϵ_{ion} and ϵ_{dis} , increase linearly to the value ϵ_1 in a time τ_{incr} , and remains at this value during a time τ_{flash} . Then, the flux level is assumed to decrease exponentially with a characteristic time τ_{decr} to the background value ϵ_0 for the ionizing flux, and to ϵ_2 for the dissociating flux. This kind of flux variations are expected in the case when the radiation pulse is assumed to be produced by an intense but short event of stellar formation or by the radiation coming from a front shock. In a few million years after the end of the stellar formation process, the ionizing flux is expected to decrease to background values. On the other hand, due to the contribution of intermediate and low mass stars to the dissociating flux, it is expected that its level remain higher than the background value ($\epsilon_2 > \epsilon_0$) long after the death of massive stars.

For a given initial state of the cloud, there is a critical background flux level ϵ_{cri} , bellow which the cloud spontaneously cools because the self-shielding allows the formation of H_2 at relatively high concentrations. This critical background flux level is mainly sensible to the initial ion fraction due to its strong influence on the H_2 formation rate. In order to describe this initial state dependence, it is useful to look at the thermo-chemical equilibrium (TCE) curve (i.e. $\mathcal{L} = 0$, and $\frac{dX_i}{dt} = 0$). Figure (1.a) shows the TCE curves for two different values of the background flux level (lower curve $\epsilon_0 = 1$, and upper curve $\epsilon_0 = 10$) when the mass of the cloud is $10^7 M_\odot$. Note the three phase structure characterized by the presence of three stable branches (solid lines) denoted in Fig. (1.a) as W-I (i.e. warm-Ionized; $T \gtrsim 13000\text{K}$), W-N (i.e. warm-Neutral; $8000\text{K} \lesssim T \lesssim 6000\text{K}$), and C-N (i.e. cool-Neutral; $T \lesssim 300\text{K}$). Note also the qualitative difference of the TCE curve for low ($\epsilon_0 = 1$) and high ($\epsilon_0 = 10$) background flux level. That is, for $\epsilon_0 = 10$ the left-hand maximum (denoted as P_{max-1}) is over the right-hand maximum (denoted as P_{max-2}), whereas, $P_{max-1} < P_{max-2}$ for $\epsilon_0 = 1$. This difference is important because if the cloud is initially in TCE in the W-I branch, and the pressure is progressively increased from $P < P_{max-1}$ to $P > P_{max-1}$ a transition to the W-N phase occurs in the case $\epsilon_0 = 1$, but in the case $\epsilon_0 = 10$ the C-N phase is reached. For $\epsilon_0 = 1$, Fig. (1.b) shows the typical isobaric evolution tracks for initially ionized states (arrows A, B, C and D) and for initially neutral states (arrows E, F and G). For cases A, B, and D, as expected the cloud evolves toward the stable branch W-I, W-N, and C-N, respectively. However, in case C, even when $P < P_{max-2}$ the track reaches the C-N branch transversing the W-N branch due to the inertia of the ionization fraction. More precisely, the excess of the ionization fraction shifts the maximum pressure P_{max-2} of the corresponding thermal equilibrium curve to a value bellow the pressure corresponding to case C. On the other hand, for the initially neutral states the evolution is substantially different. In case E the track stops in the W-N branch; note the difference with case C. In case F the cooling rate is so small that in practice the cloud reaches a quasi-stationary state similar to that in the W-N branch. The small cooling efficiency is due to the very small H_2 formation rate for the low ion fraction in the quasi-stationary W-N state. Finally, for high enough gas pressure as in

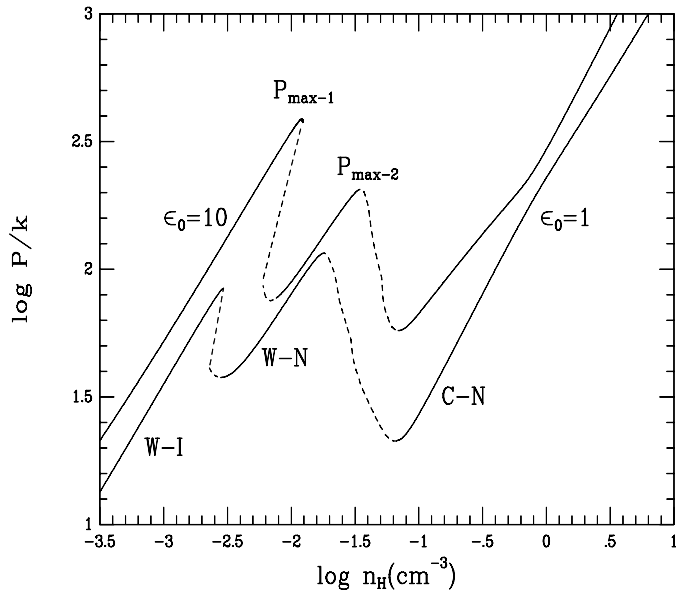


Fig. 1.a. The thermo-chemical equilibrium curves for a $10^7 M_{\odot}$ cloud exposed to the two labeled values of the background flux level (see text).

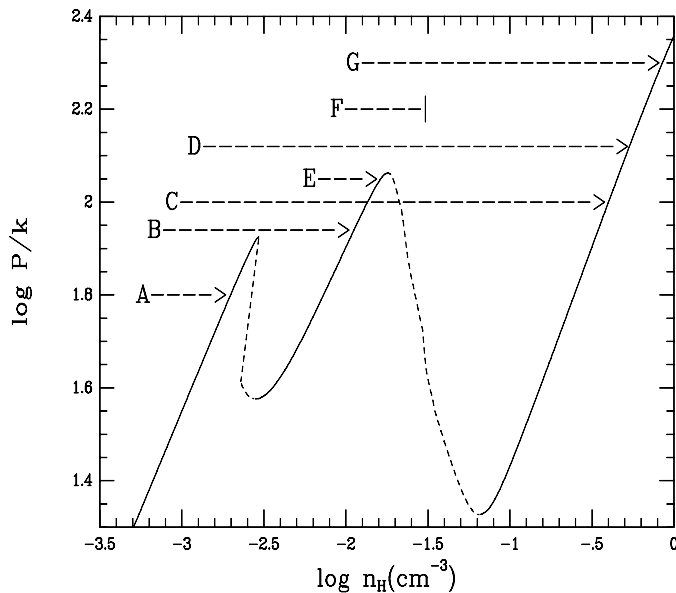


Fig. 1.b. The thermo-chemical equilibrium curve and the typical isobaric evolution tracks for initially ionized states (arrows A, B, C and D) and for initially neutral states (arrows E, F and G).

case G, the cloud reaches the C-N branch. The isobaric evolution tracks for a high background flux level (i.e. $\epsilon_0 = 10$) are similar to those in Fig (1.b) except that the W-N branch can not be reached from an ionized initial state as in case B in Fig. (1.b). It is interesting to note that when the cloud is in the quasi-stationary state schematized by track F, a large enough ionizing flash is able to increase H_2 formation rate and to stimulate the rapid condensation to reach the C-N branch.

The analysis of the various evolution tracks in Fig. (1.b) have been made for a fixed background flux level. Taken into account that an increase of the background flux level shift the TCE curve upward, a similar analysis can be made for a fixed pressure but varying the background flux level. Figure (2.a) shows, in the constant pressure approximation, the time dependence of the gas temperature for a $10^7 M_{\odot}$ cloud subject to the three labeled values of the background flux level ϵ_0 . The initial condition is the same in the three cases and corresponds to an out of equilibrium warm-ionized

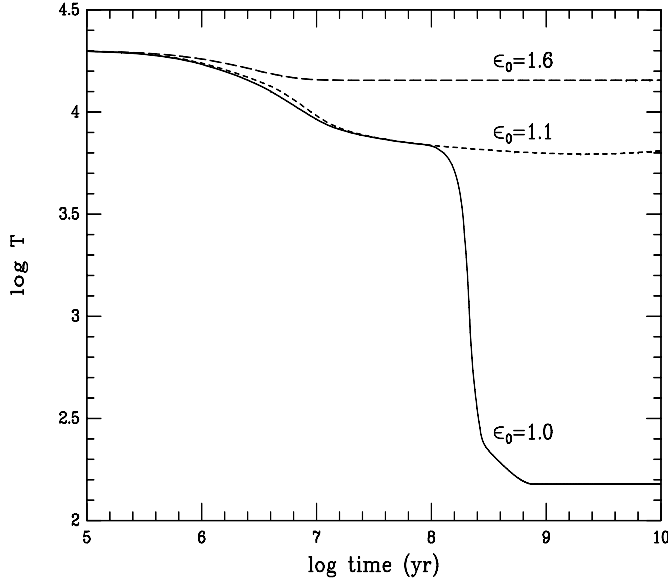


Fig. 2.a. The time dependence of the temperature for a $10^7 M_{\odot}$ cloud exposed to the three labeled values of the background flux level and an initial out of equilibrium warm-ionized state (see text).

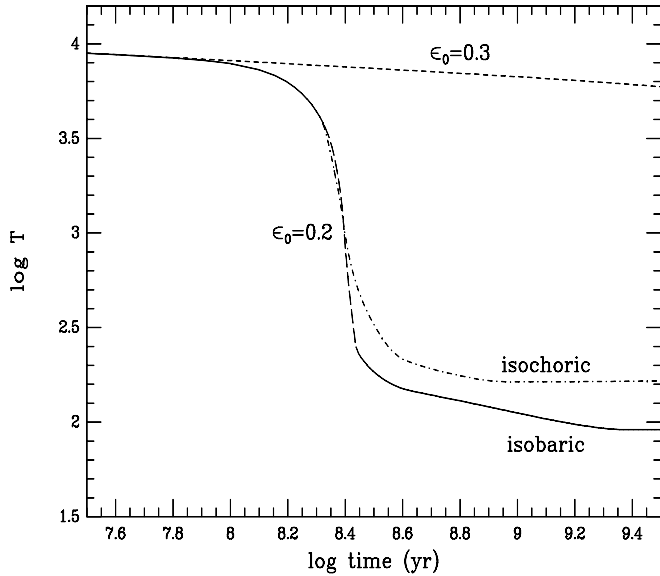


Fig. 2.b. The time dependence of the temperature for a $10^7 M_{\odot}$ cloud exposed to the two labeled values of the background flux level and an initial out of equilibrium warm-neutral state (see text).

state at a gas pressure $\log(P/k) = 2.046$, and $n = 2.5 \times 10^{-3} \text{cm}^{-3}$, $T = 2 \times 10^4 \text{K}$, $X_H = 8.8 \times 10^{-4}$, $X_{H_2} = 2.3 \times 10^{-13}$, $X_{H^+} = 0.999$, $X_e = 1.147$, $X_{H^-} = 4.6 \times 10^{-11}$, $X_{H_2^+} = 1.2 \times 10^{-11}$, $X_{He} = 2.57 \times 10^{-6}$, $X_{He^+} = 3.11 \times 10^{-3}$, and $X_{He^{++}} = 7.24 \times 10^{-2}$. The temperature evolution in the three plotted cases differs because for $\epsilon_0 = 1.6$ the system stabilizes in the W-I branch (i.e. as in track A of Fig. (1.b)), for $\epsilon_0 = 1.1$ the system stabilizes in the W-N branch (i.e. as in track B of Fig. (1.b)), and for $\epsilon_0 = 1.0$ the system stabilizes in the C-N branch (i.e. as in track C of Fig. (1.b)). On the other hand, Fig. (2.b) shows the temperature evolution for the same pressure as in Fig. (2.a), but for an initially neutral warm state, (i.e. $n = 1.0 \times 10^{-2} \text{cm}^{-3}$, $T = 1.03 \times 10^4 \text{K}$, $X_H = 0.9992$, $X_{H_2} = 5.801 \times 10^{-7}$, $X_{H^+} = 7.978 \times 10^{-4}$, $X_e = 2.631 \times 10^{-3}$, $X_{H^-} = 3.914 \times 10^{-8}$, $X_{H_2^+} = 4.813 \times 10^{-9}$, $X_{He} = 7.374 \times 10^{-2}$, $X_{He^+} = 1.819 \times 10^{-3}$, and $X_{He^{++}} = 7.169 \times 10^{-6}$). In this case, the evolution for $\epsilon_0 = 0.3$ corresponds to the situation schematized by track F in Fig. (1.b); that is, the system enters in a quasi-stationary state characterized by a very slow decrease of the

temperature. However, for $\epsilon_0 = 0.2$ the system evolves rapidly to the C-N branch, a situation that corresponds to that schematized by track G in Fig. (1.b). The results in Figs. (2.a) and (2.b) illustrate how the initial cloud state affects the critical value of ϵ_0 below which the cloud evolves toward the C-N branch (i.e. the cloud condenses). In order to show the effect of the constant density approximation, Fig. (2.b) also shows the temperature evolution for $\epsilon_0 = 0.2$ when the constant pressure approximation is switched to the constant density approximation at the time when the rate of decrement of the cloud radius equals the sound speed.

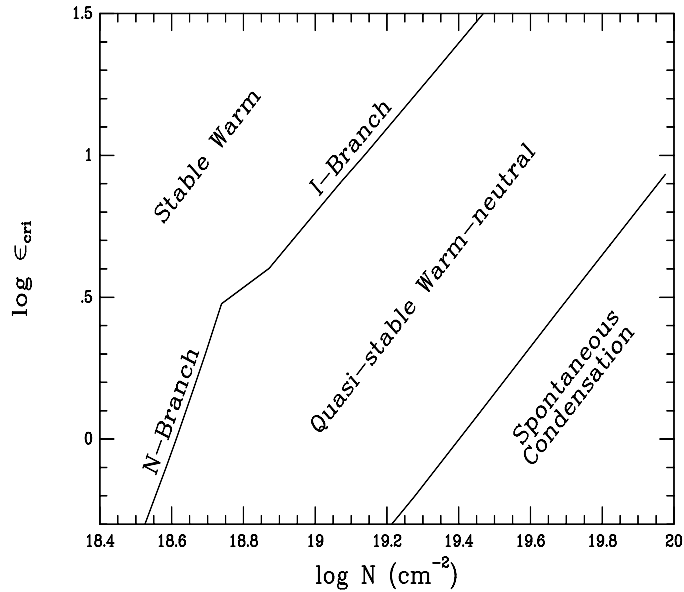


Fig. 3. The dependence of ϵ_{cri} on the initial cloud column density (see text).

For initially ionized states at pressure P , the critical value ϵ_{cri} roughly corresponds to the value of ϵ_0 that produces a maximum in the TCE curve at pressure P . For a high background flux level, the left-hand maximum (denoted as P_{max-1} in Fig. (1.a)) is the higher maximum and must be equaled to P . For a low background flux level, the right-hand maximum must be equaled to P . On the other hand, for initially neutral states, the critical value ϵ_{cri} must be calculated by finding the value of ϵ_0 below which the evolution does not fall in the quasi-stationary warm-neutral state. The dependence of the critical value of ϵ_{cri} on the initial cloud state is summarized in Fig. (3) for a $10^7 M_\odot$ cloud. The results are showed as function of the initial cloud column density ($N = n \times R_{cloud}$). The left-hand side curve corresponds to the critical background flux level for initially ionized states. The upper segment (labeled I-branch) corresponds to background flux levels for which $P_{max-1} > P_{max-2}$, and therefore, the condition $P_{max-1}(\epsilon_{cri}) = P$ is used. The lower segment (labeled N-branch) corresponds to the case when the condition $P_{max-2}(\epsilon_{cri}) = P$ is used because $P_{max-2} > P_{max-1}$ for these values of ϵ_{cri} . The initial column density is calculated assuming that initially the cloud is at $2.0 \times 10^4 K$ and at a pressure $P = P_{max}(\epsilon_{cri})$; the initial concentrations are assumed to be the used in Fig. (2.a). For values of (N, ϵ_0) above the left-hand $\epsilon_{cri}(N)$ curve, the initially ionized cloud reaches TCE in the stable warm phase, but below this curve the cool-neutral branch is reached. On the other hand, the right-hand side curve corresponds to the critical background flux level for initially neutral states. In this case, the initial column density is calculated assuming that initially the cloud is at $1.2 \times 10^4 K$ and the initial concentrations are assumed to be the used in Fig. (2.b); the initial density is varied in order to cover the plotted range of ϵ_{cri} . For values of (N, ϵ_0) above the right-hand $\epsilon_{cri}(N)$ curve, the initially neutral cloud attains a quasi-stationary warm-neutral state, but below this curve the cool-Neutral branch is reached. It is to be noticed that as the initial electron concentration increase, the right-hand $\epsilon_{cri}(N)$ curve approaches the left-hand curve. In any case, there exist a set of initial conditions for which the cloud reaches a quasi-stationary warm-neutral state. The point to be emphasized is that these quasi-stationary states are susceptible to be induced to condensate if the cloud is exposed to an intense enough ionizing flash.

In order to illustrate the effect of the ionizing flash on a cloud that has fallen in the quasi-stationary warm-neutral state, Figs. (4a,b,c) show respectively the time dependence of the temperature, the relative number density of electrons (X_{e-}), and of Hydrogen molecules (X_{H_2}), for a $10^7 M_\odot$ cloud. The initial condition corresponds to an out of equilibrium warm-neutral state at a gas pressure $\log(P/k) = 2.074$ (i.e. $n = 1.1 \times 10^{-2} cm^{-3}$, $T = 1.0 \times 10^4 K$,

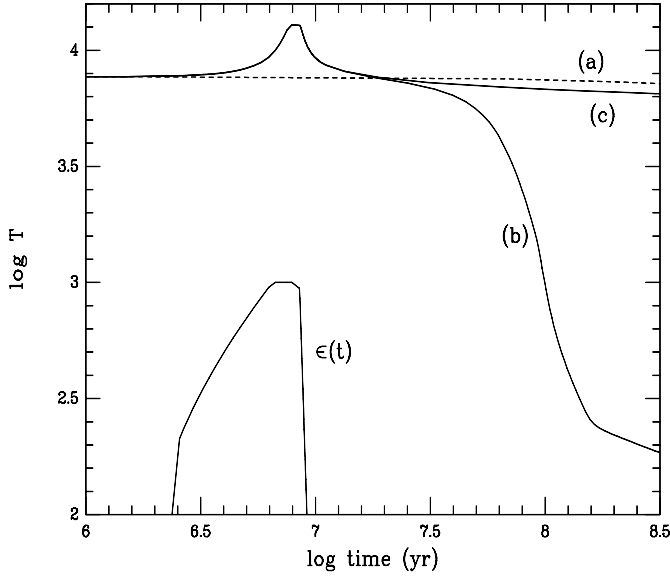


Fig. 4a. The effect of the ionizing flash $\epsilon(t)$ on the the time dependence of the temperature for a $10^7 M_{\odot}$ cloud. The curve labeled (a) corresponds to the case $\epsilon(t) = \epsilon_0 > \epsilon_{cri}$. The curves labeled (b) and (c) correspond to the evolution of the cloud when it is subjected at $t = 2 \times 10^8$ yr to a flash (see text).

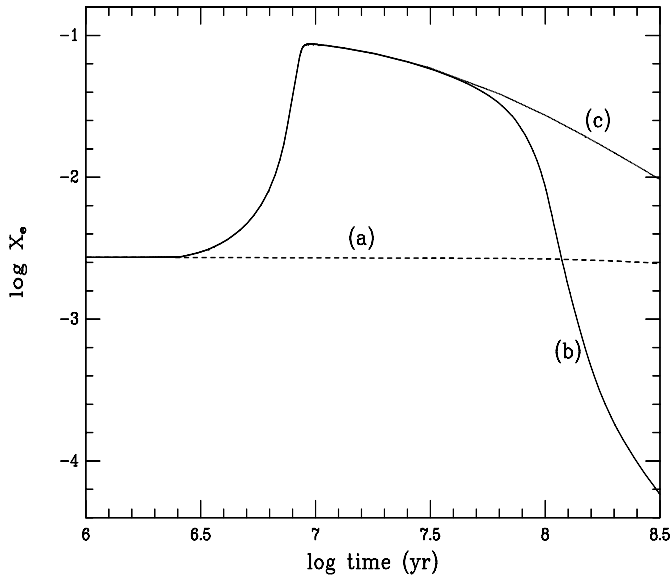


Fig. 4b. The time dependence of the relative number density of electrons (X_{e^-}) for the initial and external conditions corresponding to Fig. (4a).

and the initial concentrations used in Fig. (2.a)). The curves labeled (a) in Figs. (4) are plotted for reference, and correspond to the case when the cloud is subject to a constant background flux level of $\epsilon_0 = 1.0$. As expected for $\epsilon(t) = \epsilon_0 > \epsilon_{cri}$, the cloud evolves toward a quasi-equilibrium warm neutral state. The curves labeled (b) and (c) in Figs. (4) correspond to the evolution of the cloud when it is subjected at $t = 2 \times 10^8$ yr to a flash. In case (b), the flash characteristics are: $\tau_{incr} = 5 \times 10^6$ yr, $\tau_{flash} = 2 \times 10^6$ yr, $\tau_{decr} = 2 \times 10^6$ yr, $\epsilon_1 = 10^3$, and $\epsilon_2 = 1.5 \times \epsilon_0$. In case (c) the flash characteristics are the same as in case (b) but with $\epsilon_2 = 2 \times \epsilon_0$. Notice in Figs. (4) that during the increase of the external radiation flux from ϵ_0 to ϵ_1 , the electron density and the temperature increase, whereas the H_2 and H^- densities decrease. During the time when $\epsilon(t) = \epsilon_1$, the electron density and the temperature continue to increase because the variation of $\epsilon(t)$ during the time τ_{incr} is rapid enough to leave the gas far from equilibrium.

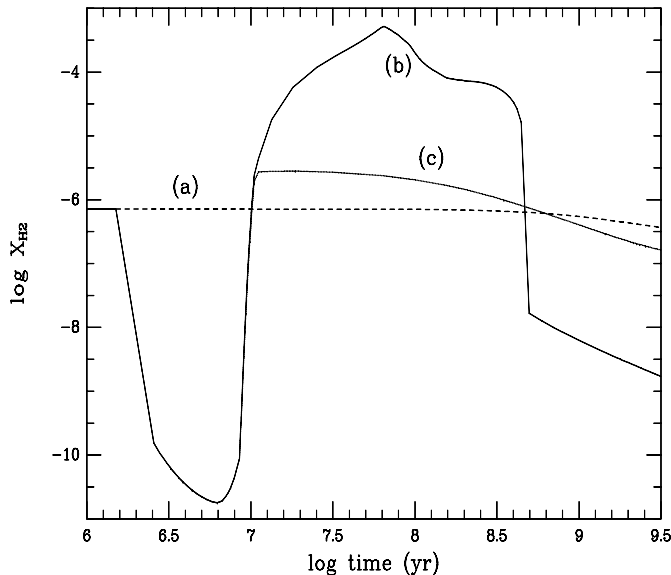


Fig. 4c. The time dependence of the Hydrogen molecules (X_{H_2}), for the initial and external conditions corresponding to Fig. (4a).

At the end of the lapse of decrement of $\epsilon(t)$, if τ_{decr} is short enough, the gas has an excess of electrons and thermal energy compared with the equilibrium values corresponding to $\epsilon_{ion} = \epsilon_0$ and $\epsilon_{diss} = \epsilon_2$. After the lapse of UV flux decrement, recombination continues, but at a lower rate than the cooling. The excess of electrons at these relatively low temperatures results in an enhancement of the H_2 rate formation. Even when $\epsilon_2 > \epsilon_0$, the abundance of H_2 may reach a large enough value to produce considerable self-shielding. If the cloud reaches a critical value ($\tau \sim 1$) for the optical depth at dissociating frequencies, the H_2 abundance grows very fast, allowing the cooling of the cloud to temperatures of the order of 100K. This is the situation for case (b) in Figs. (4), where the flash induce rapid cooling even when $\epsilon_2 = 1.5 \times \epsilon_0$. On the other hand, for case (c) a post flash dissociating level with $\epsilon_2 = 2 \times \epsilon_0$ is enough to inhibit the formation of H_2 , and then, the cloud remains warm.

A detailed study of the dependence of the cloud evolution on the phase space of free parameters (cloud mass, initial conditions, and flash characteristics) is out of the scope of this simple application. However, such detailed study may reveal that the stimulating condensation process studied here can be effective in a restricted region of the free parameters space, and therefore, may act as a selective effect that contributes to the formation of dense structures at certain scales.

4. Ionizing pulse as trigger of warm to cool phase transition in a gas with solar abundances

Among the various processes that determine the change of state of the ISM material, phase transitions are expected to play an important role. In particular, warm to cool phase transition has been indicated as a channel to transform diffuse gas ($< 10^{-1} \text{cm}^{-3}$) into denser states ($> 10^1 \text{cm}^{-3}$) (Field, Goldsmith & Habing 1969; Lepp et al. 1985; Parravano 1987; Lioure & Chièze 1990; Dickey & Brinks 1993). Moreover, it has been proposed (Parravano 1988, 1989) that the large scale star formation rate must be self-regulated because, on one hand the warm gas condensation is inhibited by high enough UV radiation (coming mainly from massive stars), and on the other hand, a gas supply from the diffuse phases is required to feed the large scale star formation process. In this way, the large scale star formation rate is limited, and the warm gas tends to remain close to the critical state for warm to cool phase transition. The fact that large quantities of ISM warm gas remain close to this critical state allows the trigger of condensation by relatively small variations of the ambient conditions. More precisely, the mean “distance” of the warm gas state to the critical state for spontaneous condensation is determined by the amplitude spectrum of the variations of the ambient conditions. In any case, the study of triggered condensation of warm gases close to the critical state can be justified by the self-regulatory hypothesis. It is to be noticed that the scale of the inhibitory process is expected to be much larger than the scale of the triggering processes: a fact that apparently is a common characteristic of many dynamical systems where spiral structures arise (Smolin 1996).

Triggering mechanisms of star formation are usually related to compression and pushing of the ISM gas by high pressure events associated to stars formed previously (reviews on this topic can be found in Elmegreen 1992, Franco 1992). Also, compression of the warm gas by the spiral density wave have been evocated as a main trigger of its condensation (Roberts 1969); however, stimulated condensation by ionizing flashes may also enter as an initiator of the chain of processes that finally results in the formation of stars. As it will be shown bellow, this stimulating mechanism is particularly efficient when the warm gas state is close to its marginal state for spontaneous phase transition. Moreover, variations of the ionizing flux are expected to precede pressure variations if both variations are associated to the same perturbing event. Large local variation of the ionizing rate are expected to be present in the interstellar medium. Sudden appearance and disappearance of ionizing sources occur continuously in the galactic plane. Also, “rapid” variation of the opacity to the ionizing radiation in a line of seeing is expected. Finally, variations of the cosmic ray flux are expected to be present due to variations of the sources (cosmic ray acceleration in shock fronts with oblique B-fields; Blandford and Ostriker 1978), and to variations of the magnetic field topology (i.e. focalization or dis-focalization of the cosmic ray stream in a region). It was also proposed (Ko & Parker 1989; Nozakura 1993) that star formation controls dynamo activities and hence large scale magnetic fields of disk galaxies.

The cooling of the diffuse warm interstellar gas is mainly due to electron collisional excitation of a) fine structure levels and metastable states of the positive ions C^+ , Si^+ , Fe^+ , and S^+ , and b) Ly_α excitation. Therefore, an increase of the ionizing flux (and the consequent increase of the electron density) tends to reduce the gas temperature if the increase of the cooling efficiency overcomes the associated increase of the heating. In general, this is the case for low equilibrium ionization fractions when the kinetic energy of the electrons that result from the ionization process is small. Depending on the value of the pressure and on the increase of the ionizing flux, the new thermal equilibrium state might be located in the cool neutral branch. That is: sufficiently large variations of the ionizing rate are expected to provoke the warm to cool phase transition. Moreover, if the ionizing flux variation has a flash-like variation, then, after the passing of the flash, the cooling rate remains enhanced due to the inertia of ionization.

In order to illustrate this effect, we consider variations of the primary ionization rate by cosmic rays ζ_o which is the accepted main source of ionization of the interstellar warm gas far away from massive stars. Other mechanisms of ionization have been proposed (i.e. OB stars (Reinolds & Cox 1992), the neutrino decay theory (Sciama 1990, 1993)), but for the present analysis the exact mechanism of ionization is not relevant. What is important here is the variation of the ionizing and heating rates due to a change of the considered ionizing flux.

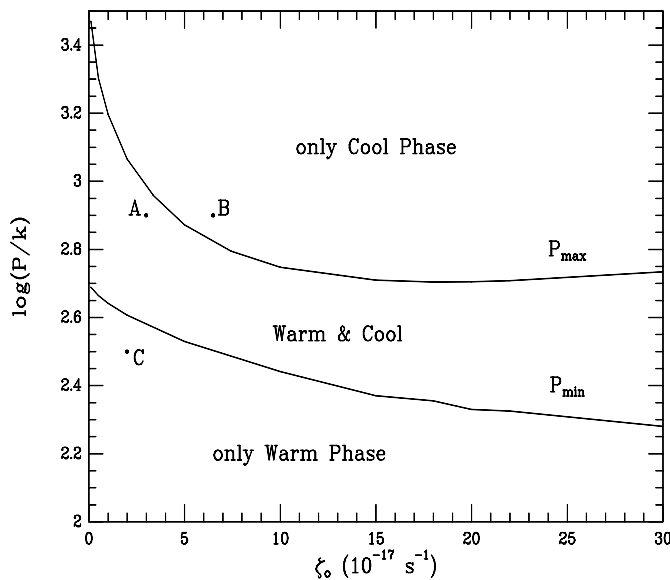


Fig. 5. The maximal (P_{max}) and the minimal (P_{min}) pressures of the thermo-chemical equilibrium curve plotted as a function of ζ_o (see text).

The main changes of the curve of thermo-chemical equilibrium (TCE) when ζ_o is changed are summarized in Fig. (5), where the maximal (P_{max}) and the minimal (P_{min}) pressures of the TCE curve are plotted as a function of ζ_o . All the results in this section correspond to the standard solar neighborhood far UV energy density and gas composition.

The labels are used to remind that if $P < P_{min}$ (or $P > P_{max}$) then there is only one possible state of TCE in the diffuse and warm phase (or in the dense and cool phase). If $P_{min} < P < P_{max}$ then the gas may reach any of the two stable branches (the warm or the cool branch). If the gas is initially in TCE at the warm branch (for example with the external conditions (P_o, ζ_{oA}) corresponding to the point (A) in Fig. (5), then, the gas could be forced to evolve toward the cool branch if the external conditions are changed, for example, to (P_o, ζ_{oB}) corresponding to the point (B). The typical time for the transition from the warm to the cool branch is $\sim 10^7$ yr. Once the gas reaches the cool phase, the external conditions can change again to (P_o, ζ_{oA}) but the gas will remain in the cool branch. To drive the gas to the warm phase again, the external conditions must be changed, for example, to (P_{oC}, ζ_{oC}) corresponding to the point (C) in Fig. (5). Now, the gas could return to the initial state if the external conditions changes to the initial condition (P_o, ζ_{oA}) .

The phase transitions described above assume that the time between the consecutive changes of ζ_o are long enough to reach TCE. If the variation of ζ_o occurs before TCE is achieved, then, the phase transition does not necessarily occur. Here we will consider the effect of flash-like variations of ζ_o at constant pressure. That is, at the beginning we assume that the gas is in the warm branch in the equilibrium state corresponding to the external conditions (P_o, ζ_{oa}) . Then, ζ_o is increased abruptly by a factor F_z during a lapse of time Δ_t , after which the primary ionization rate by cosmic rays returns to the initial value ζ_{oa} . As mentioned above, a fact that favors the phase transition is that the recombination time is much larger than the cooling time; then after the end of an ionizing pulse, the cooling rate remains enhanced due to the non-equilibrium excess of electrons.

In this simple analysis we neglect non-local processes as thermal conduction, cosmic ray attenuation, radiative transfer, and gas dynamics. Only local processes of radiative cooling, heating, H ionization and recombination are considered (Parravano 1986), assuming that the pressure remains constant during evolution. The neglected non-local processes may play an important role in the local evolution of the gas and in should determine the spatial variations of the physical variables. However, here we are interested in showing that the inertia of ionization (after the passing of the ionizing pulse) can, in many cases, enhance sufficiently the cooling efficiency to produce a phase transition from the warm gas phase to the cool phase. The evolution of the temperature and the ionization degree is calculated by solving simultaneously the energy conservation equation (2), and the kinetic equation (1) restricted to the Hydrogen ionization-recombination processes.

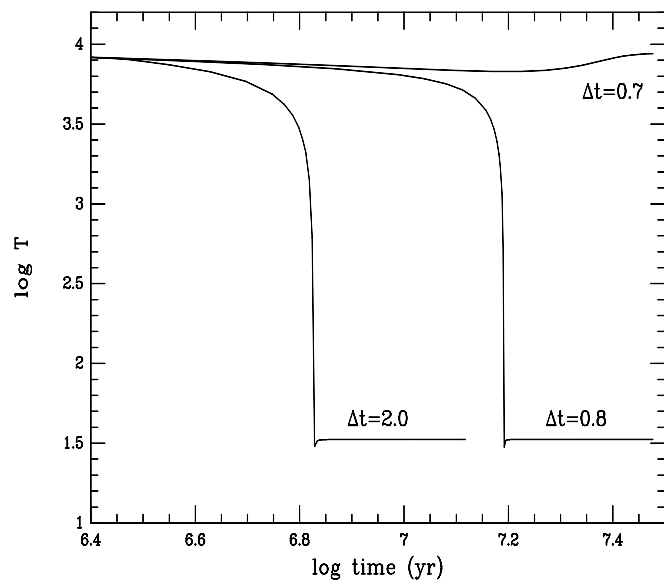


Fig. 6. The temperature evolution of the warm gas initially in thermo-chemical equilibrium close to the critical state for spontaneous condensation. The three curves correspond to the evolution for three labeled values of the pulse duration when $F_z = 20$.

In order to show the effect of ionizing pulses, Fig. (6) shows the evolution at constant pressure of a warm gas initially in thermo-chemical equilibrium close to the critical state for spontaneous condensation. The pressure P_o is below P_{max} by a factor $\eta = P_o/P_{max}(\zeta_{oo}) = 0.8$, when the pre-flash primary ionization rate is $\zeta_{oo} = 10^{-17}\text{s}^{-1}$. The three curves in Fig. (6) correspond to the evolution for three different values of the pulse duration $\Delta_t = 0.7, 0.8$, and

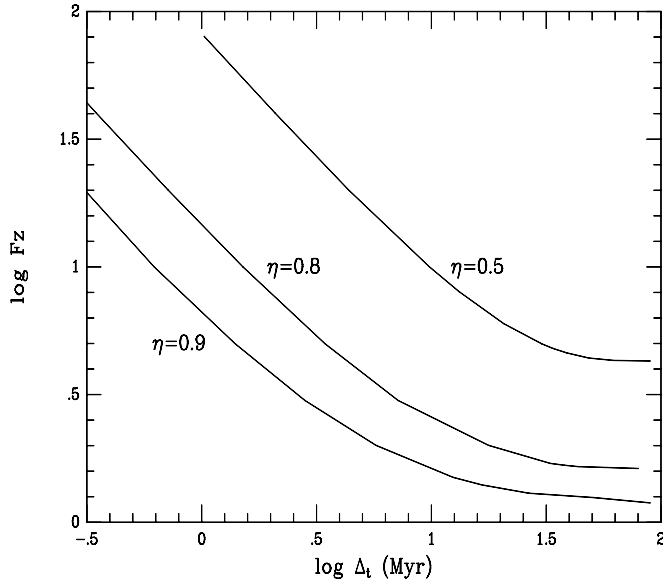


Fig. 7. The critical values of F_z as function of Δ_t for the three labeled values of η .

2.0 Myr, when the flash is initiated at $t = 10^6$ yr and the factor of increment of ζ_o is $F_z = 20$. Note in Fig. (6) that there is a critical value of Δ_t below which condensation does not occur (in this case ~ 0.7 Myr). Note also that the time required to complete the phase transition decreases as Δ_t increase, but the time required for the temperature drop from $\sim 5000\text{K}$ to $\sim 50\text{K}$ is insensitive to Δ_t . The kink at the bottom of the $\Delta_t = 0.8$ and 2.0 curves, and the smooth dip in the $\Delta_t = 0.7$ curve are due to the inertia of the ionization fraction (the recombination time is much longer for the conditions corresponding to the upper curve).

In Fig. (7) the critical values of F_z are plotted as function of Δ_t for the three labeled values of η . These curves divide the plane (F_z, Δ_t) in two regions: above the curves the flash is capable of inducing phase transition, and below the curve the gas returns to its initial state after the passing of the flash. Note that a cosmic ray pulse with a factor of increment F_z of the order of 10, and a duration of about one Myr can induce the condensation of the warm gas in TCE at $\eta > 0.8$.

5. Summary and Conclusions

The variation of the ionizing flux as a mechanism for stimulating the condensation of the diffuse gas was considered. To illustrate this effect, two situations were examined: one on the context of pregalactic conditions (a free metal cloud), and the other on the context of the actual interstellar medium (a gas with solar abundances). We have focused our attention on flash-like variations; that is, during a “short” period of time the ionizing flux is enhanced in comparison to the pre and post flash values. In both cases the cause of the induced phase change is the same: the enhancement of the cooling rate by the increase of the electron density caused by the momentary increase of ionizing flux. After the passing of the flash, the cooling rate remains enhanced due to the inertia of the ionization. In the first case (metal free gas) we show that after the lapse of UV flux decrement, recombination continues, but at a lower rate than the cooling. The excess of electrons at these relatively low temperatures results in an enhancement of the H_2 rate formation due to the enhanced abundance of the H^- intermediary. Even when $\epsilon_2 > \epsilon_0$, the abundance of H_2 may reach a large enough value to produce considerable self-shielding. If the cloud reaches a critical value ($\tau \sim 1$) for the optical depth at dissociating frequencies, the H_2 abundance grows very fast, allowing the cooling of the cloud to temperatures of the order of 100K. The temperature drop occurs in a fraction (~ 0.2) of the free fall time provoking a rapid decrease of the Jeans mass. However, if the post-flash dissociating level is large enough the H_2 formation can be inhibited and the cloud remains warm.

In the second case (solar abundances gas) the dominant cooling mechanism of the warm neutral gas (the excitation of heavy ions by electron impacts) is proportional to the electron density, and therefore, the ionizing flash increases the cooling efficiency. We consider flash-like variations of the primary ionization rate by cosmic rays and calculate the marginal flash characteristics to induce warm gas condensation. We show that, for the expected states of the warm interstellar gas, ionizing flashes may easily induce the phase transition from the warm to the cool phase. The phase

transition is completed in about 10^7 yr; however, the drop in the temperature from $\sim 5000\text{K}$ to $\sim 50\text{K}$ occurs in about 5×10^5 yr.

The results indicate that the mechanism of induced condensation studied here might play a relevant role in the gas evolution of the diffuse gas in both, the pregalactic and the actual interstellar medium conditions.

The above results include only local processes. However, non-local processes like thermal conduction impose restrictions on the size of the condensing structures. Thermal conduction tends to attenuate temperature gradients, and therefore, it imposes a minimal value for the mass of the condensing structures (Corbelli & Ferrara 1995; Ibáñez & Rosenzweig 1995; Steele & Ibáñez 1997). Critical masses of the order of galaxy masses are obtained in the case of a metal-free gas (Ibáñez & Parravano 1983) and in the case of an actual interstellar gas, masses of the order of one solar mass are obtained (Parravano 1986; Parravano, Ibáñez & Mendoza 1993). However, a wide range of critical masses are obtained depending on the initial gas state, and ambient conditions. Therefore, in addition to the restrictions on F_z and Δ_t to induce the warm gas condensation, the cosmic ray flash should cover a region greater than the critical value imposed by thermal conduction and other diffusive processes.

Acknowledgements. We are very grateful to the referee A. Ferrara for his useful comments that motivated us to include Helium in the metal free model and to clarify the discussion by including the phase diagram. This work has been supported by CDCHT and calculations were performed at CECALCULA, both institutions of the Universidad de Los Andes.

References

- Anninos P., Norman M.L., 1996, *Apj* 460, 556
 Blandford R.D., Ostriker J.P., 1978, *Apj* 221, L29
 Cammerer M., Shchekinov Yu., 1994, *A&A* 283, 845
 Commins N.F., Shore S.N., 1990, *A&A* 237,345
 Corbelli E., Ferrara A., 1995, *Apj* 447, 708
 Cox D.P., 1985, *Apj* 288, 465
 Dickey J.M., Brinks E., 1993, *Apj* 405, 163
 Donahue M., Shull J.M., 1991, *Apj* 383, 511
 Elmegreen B.G., 1992, in: *Star formation in Stellar Systems*, eds. G. Tenorio-Tagle, M. Prieto, F. Sanchez, Cambridge University Press, p. 381
 Fall S.M., Rees M.J., 1985, *Apj*. 298, 18
 Field G.B., Goldsmith D.W., Habing H.J., 1969, *Apj* 155, L149
 Ferrara A., Giallongo E., 1996, *MNRAS* 282, 1165
 Franco J., 1992, in: *Star formation in Stellar Systems*, eds. G. Tenorio-Tagle, M. Prieto, F. Sanchez, Cambridge University Press, p. 515
 Gerola H., Seiden P.E., 1978, *Apj* 223, 129
 Haardt F., Madau P., 1996, *Apj* 461, 20
 Haiman Z., Rees M.J., Loeb A., 1996, *Apj* 467, 522
 Ibáñez S.M.H., Parravano A., 1983, *Apj* 275, 181
 Ibáñez S.M.H., Rosenzweig P., 1995, *Phys. Plasmas* 11, 4127
 Izotov Yu.I., 1989, *Kiev Inst. Teoret. Fiz. ITP-89-17E*
 Izotov Yu.I., Kolesnik I.G., 1984, *Soviet Astr.* 28, No 1, 15
 Kang H., Shapiro P.R., Fall S.M., Rees M.J., 1990, *Apj* 363, 488
 Kapral R., 1993, in: *Theory and applications of coupled map lattices*, ed. K. Kaneko, John Wiley & Sons Ltd, p. 135
 Klonover A., Kaldor U., 1979, *J. Phys. B* 12, 3797
 Ko C.M., Parker E.N., 1989, *Apj* 341, 828
 Lepp S., McCray R., Shull J.M., Woods D.T., Kallman T., 1985, *Apj* 228, 58
 Lepp S., Shull J.M., 1983, *Apj* 270, 578
 Lioure A., Chièze J-P., 1990, *A&A* 235, 379
 Mucket J.P., Kates R.E., 1997, submitted to *A&A*, preprint astro-ph/9702022.
 Murray S.D., Lin D.N.C., 1990, *Apj* 363, 50
 Navarro J.F., Steinmetz M., 1996, submitted to *Apj*, preprint astro-ph/9605043
 Nozakura T., 1993, *MNRAS* 260, 861
 Padoan P., Jimenez R., Jones B., 1996, submitted to *MNRAS*
 Palla F., Stahler S.W., 1983, *Apj* 271,632
 Palla, F., and Zinnecker, H. 1987, in: *Starbursts and Galaxy evolution*, ed. T.X. Thuan, T. Montmerle, and J. T. Thanh Van (Gif Sur Yvette: Editions Frontières),p. 533
 Palouš J., Franco J., Tenorio-Tagle G., 1990, *A&A* 283,845
 Parravano A., 1987, *A&A* 172, 280
 ———— 1988, *A&A* 205, 71

- Parravano A., Ibáñez S.M.H., Mendoza B.C.A., 1993, *Apj* 412, 625
Reinolds R.J., Cox D.P., 1992, *Apj* 400, L33
Roberts W.W., Jr., 1969, *Apj* 158, 123
Rosenzweig P., Parravano A., Ibáñez S.M.H., Izotov Yu.I., 1994, *Apj* 432, 485
Sciama D.W., 1990, *Apj* 364, 549
——— 1993, *Apj* 409, L25
Seiden P.E., Gerola H., 1982, *Fund. Cosmic. Phys.* 7, 241
Shapiro P.R., Kang H., 1987, *Apj* 318, 32
Shore S.N., 1981, *Apj* 249,93
——— 1983, *Apj* 265, 202
Smolin L., 1996, astro-ph/9612033 preprint
Steele C.D.C., Ibáñez S.M.H., 1997, submitted to *Phys. Plasmas*
Tegmark M., Silk J., Rees M.J., Blanchard A., Abel A., Palla F., 1996, *Apj* 474, 1